An Overview of Coronal Seismology and Application to Data from AIA/SDO

Laurel Farris*, R. T. James McAteer*

New Mexico State University

Introduction & motivation

The method of coronal seismology involves the observation and characterization of disturbances in the solar corona. Such disturbances can be in the form of standing oscillations in coronal structures or waves propagating across the surface and through the atmosphere between the photosphere and corona. These disturbances can be triggered by a variety of phenomena, such as the continuous motions of the photosphere around the footpoints of coronal loops, or the impulsive burst of motion from a flare or coronal mass ejection (CME). The characteristics of the waves produced by this activity can reveal information about the flares/CMEs themselves. Coronal seismology also offers a way to extract coronal parameters that are difficult to observe directly, such as magnetic field strength.

Magnetohydrodynamics (MHD)

Figure 1: A typical coronal loop

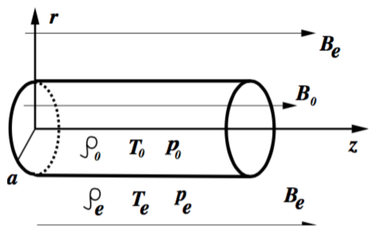

Figure 2: Cylindrical model of a waveguide

Coronal seismology is based on the theories of ideal magnetohydrodynamics (MHD), where waves and oscillations in the corona are modelled as propagating in a uniform magnetic field, guided by a straight cylindrical flux tube (figure 2). Coronal loops, such as the one pictured in figure 1, can act as a waveguide, and are just one of the structures in the corona that support MHD modes. These modes are Characterized by different wave speeds that are determined by the gas density (ρ), gas temperature (T), gas pressure (P), and magnetic field strength ($\vec{B}$), both interior and exterior to the waveguide (see figure 2 at left). Two of the more familiar characteristic speeds are:

Sound speed $C_s \propto \sqrt{\frac{P}{\rho}} \propto \sqrt{T}$

Alfvén speed $V_A \propto \frac{B}{\sqrt{\rho}}$

Other structures that can support MHD modes include sunspot pores and magnetic bright points. A bright point in a coronal hole is analyzed for this project (see Data and subsequent sections).

Coronal Seismology

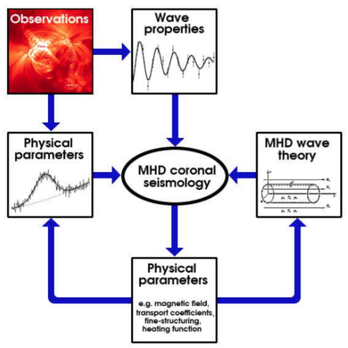

Figure 3: Schemetic of how physical properties and wave properties are connected by coronal seismology.

The method of coronal seismology can be summarized in four steps:

1. Observe disturbances
2. Measure physical parameters
3. Identify wave properties
4. Extract physical parameters

How these disturbances are observed depends on a number of factors: direction of travel relative to the line-of-sight, whether or not they show visible variations (such as intensity changes, which correspond to density changes in the plasma), and whether the spatial variations occur on sizescales for which sufficient resolution is available. Figure 3 shows how direct observations of physical properties and extracted properties are interrelated throught coronal seismology.

MHD wave modes

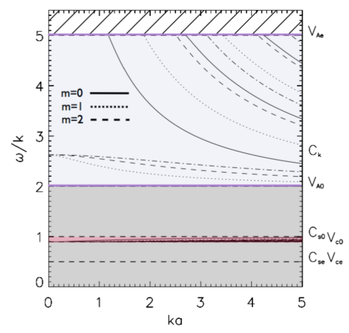

Figure 4: Dispersion diagram for MHD modes

Figure 4 shows the phase velocities (ω/k), expressed as multiples of the internal sound speed (C_0) of the waveguide, as functions of wavenumber (ka) for different types of MHD modes. In general, MHD modes are categorized as follows:

Magnetoacoustic Analagous to regular acoustic waves, (or sound waves), these are pressure-driven waves in the presence of a magnetic field. They are sub-divided into two more groups:

- **Fast** Phase speeds faster than the internal Alfvén speed (V_{A0}).
- **Slow** Phase speeds close to the internal sound speed (C_0).

Alfvén These are magnetically driven waves, with speeds determined by $\vec{B}$.

Data

Some of the techniques of coronal seismology were tested on a series of images from the Atmospheric Imaging Assembly (AIA) instrument on board the *Solar Dynamics Observatory (SDO)*, at the 193 Å line (Fe XII and Fe XXIV). This line occurs at temperatures of around 10^6 K. The data set spanned one hour in July of 2012 and were taken at a cadence of 12 seconds, for a total of 300 images. The first image in the series is shown in figure 5.

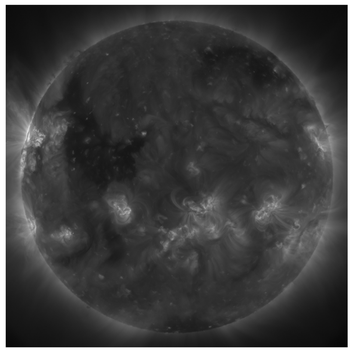

Figure 5: First image in the time-series from AIA/*SDO*

The full disk shows an active region in the lower right, a coronal hole in the upper left, and some quiet sun areas in the upper right. A bright point from the coronal hole was selected for analysis, and is shown in figure 6.

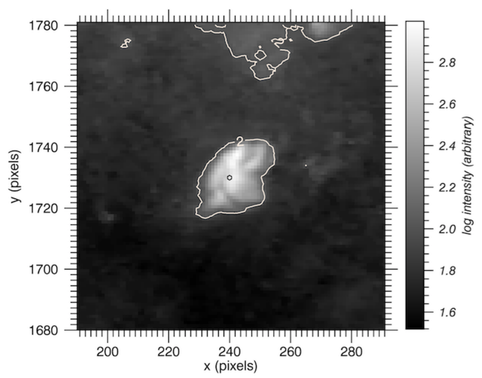

Figure 6: Image of the single bright point analyzed for this project.

The contours around the bright point outline its estimated physical boundary, which was determined using an intensity cutoff. The areas in the upper region of the image were also above this intensity threshold, and therefore are also outlined. The circle in the center indicates the location of the pixel that was correlated with every other pixel in the image (see Analysis techniques).

Analysis techniques

Two general analysis techniques were applied to this data set:

Lightcurves The variation in intensity of the bright point, along with the size as determined by the intensity threshold, are both plotted in figure 7 as functions of time. The phase difference between intensity and size can be an indication of the type of MHD mode (for instance, the so-called "sausage modes" have a characteristic phase difference equal to π between the two).

Cross-correlation To search for patterns in the horizontal direction (i.e. across the surface at the same height), a cross-correlation was calculated between the central pixel in the bright point and every other pixel in figure 6 across the time-series. With this technique, the distance, speed, and/or oscillation period of a disturbance traveling outward from the brightpoint could be potentially be extracted.

Lightcurve results

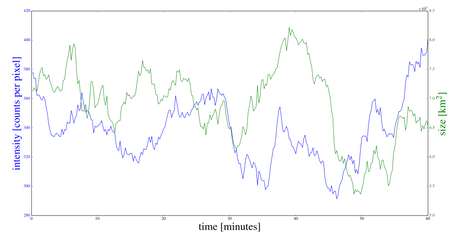

Figure 7: Size and intensity of the bright point as functions of time throughout the entire data series.

Figure 7 shows how the size and intensity (per unit area) varied over the course of one hour. There appears to be a similar pattern between the two; they become closer in phase at the end of the time series. Further numerical analysis, such as a fourier transform, is needed to extract periodicities and draw more conclusive results.

Cross-correlation results

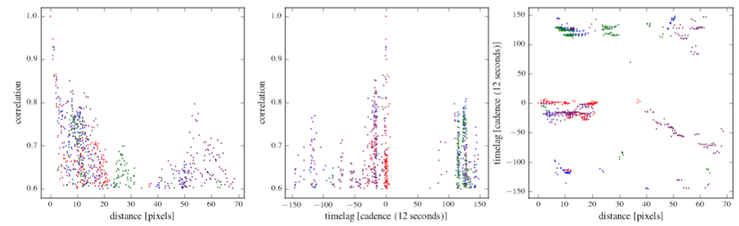

Figure 8: Relationship between the cross-correlation, timelag, and radial distance from central pixel.

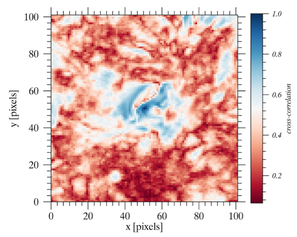

Figure 9: Image illustrating the maximum correlation value of each pixel with the central pixel.

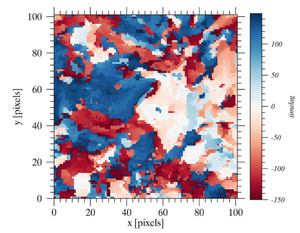

Figure 10: Image of the timelag corresponding to each correlation value in figure 9.

After running the cross-correlation, the highest values were plotted as functions of both timelag and distance. Additionally, the timelag was plotted as a function of distance. All three plots are shown in figure 8. The value of the maximum correlation value of each pixel with the central pixel is illustrated as an image in figure 9. The corresponding timelag at which each of these correlation values occurred is similarly illustrated in figure 10.

Conclusions & Future Work

Some additional calculations are required for more conclusive results: a fourier transform on the plots in figure 7 is needed to extract potential periodic information. Data from the Helioseismic and Magnetic Imager (HMI) on *SDO* during the same time as the data used here could reveal information about the magnetic counterpart to the bright point in the photosphere. There are many bright points in the coronal hole, along with quiet sun areas and active regions to look at as well.

Acknowledgements

Thanks to my advisor, Dr. James McAteer for guidance throughout this project.

References

Figure 1 is from http://scied.ucar.edu/sun-coronal-loops. Figures 2, 3, and 4 are from Nakariakov & Verwichte (2005).